JVI Journals.ASM.org

Maintenance of the Flip Sequence Orientation of the Ears in the Parvoviral Left-End Hairpin Is a Nonessential Consequence of the Critical Asymmetry in the Hairpin Stem

Lei Li,[a] Susan F. Cotmore,[a] and Peter Tattersall[a,b]

Departments of Laboratory Medicine[a] and Genetics,[b] Yale University Medical School, New Haven, Connecticut, USA

Parvoviral terminal hairpins are essential for viral DNA amplification but are also implicated in multiple additional steps in the viral life cycle. The palindromes at the two ends of the minute virus of mice (MVM) genome are dissimilar and are processed by different resolution mechanisms that selectively direct encapsidation of predominantly negative-sense progeny genomes and conserve a single Flip sequence orientation at the 3′ (left) end of such progeny. The sequence and predicted structure of these 3′ hairpins are highly conserved within the genus *Parvovirus*, exemplified by the 121-nucleotide left-end sequence of MVM, which folds into a Y-shaped hairpin containing small internal palindromes that form the "ears" of the Y. To explore the potential role(s) of this hairpin in the viral life cycle, we constructed infectious clones with the ear sequences either inverted, to give the antiparallel Flop orientation, or with multiple transversions, conserving their base composition but changing their sequence. These were compared with a "bubble" mutant, designed to activate the normally silent origin in the inboard arm of the hairpin, thus potentially rendering symmetric the otherwise asymmetric junction resolution mechanism that drives maintenance of Flip. This mutant exhibited a major defect in viral duplex and single-strand DNA replication, characterized by the accumulation of covalently closed turnaround forms of the left end, and was rapidly supplanted by revertants that restored asymmetry. In contrast, both sequence and orientation changes in the hairpin ears were tolerated, suggesting that maintaining the Flip orientation of these structures is a consequence of, but not the reason for, asymmetric left-end processing.

Members of the family *Parvoviridae* have a linear single-stranded DNA genome of about 5 kb terminating in small palindromic telomeres that can fold into self-priming hairpins at each end of the viral chromosome. These hairpins, together with a few adjacent nucleotides, contain all of the *cis*-acting information required to mediate the virus's rolling-hairpin replication strategy (24). In several parvoviral genera, the terminal palindromes form part of inverted terminal repeats (ITRs), so that the same DNA origin sequence occurs at the two ends of the genome. For these viruses, both termini are resolved by the same mechanism, called "terminal resolution," which occurs with equal efficiency at both ends of the genome and ultimately results in the release and packaging of infectious progeny single strands of both polarities. One consequence of using this mechanism is that the sequence of the hairpins is inverted with each round of synthesis, creating termini in two inverted complementary sequence orientations, dubbed "Flip" and "Flop." However, species belonging to the *Parvovirus*, *Amdovirus*, and *Bocavirus* genera are heterotelomeric; that is, their genomic termini differ from each other in size, sequence, and predicted secondary structure (39), and in minute virus of mice (MVM), the type species of the genus *Parvovirus*, the two termini are known to be processed by different mechanisms and at different rates. This property confers upon their replication a marked asymmetry, which drives the encapsidation of predominantly negative-sense progeny single strands (20). While studies on MVM have revealed the mechanism underlying this asymmetry in some detail, precisely what advantages accrue from using this more complex strategy remain uncertain.

One conspicuous result of asymmetric resolution is that a single sequence orientation, Flip, is conserved in left-end hairpins of the negative-sense progeny strands of all heterotelomeric parvoviruses examined to date (2, 3, 15, 39). The left end of MVM, and likely other heterotelomeric viruses, is excised and replicated from palindromic dimer replicative-form (RF) intermediates by a complex mechanism, termed "junction resolution" (24), which generates both a closed hairpin terminus and an extended palindromic terminus, as shown in Fig. 1A (21). Since it is not clear why this elaborate asymmetric mechanism is invoked, it is possible that it exists simply to conserve a specific feature(s) of the Flip orientation that is essential for virus viability. This hypothesis has proven difficult to test directly, for example, by transfecting synthetic genomes with hairpins in the Flop orientation, because these are simply converted back to the Flip orientation by the resolution mechanism (10). However, since the sequences that generate the asymmetry reside in the origin of DNA replication embedded within the hairpin stem (8, 9), we can effectively manipulate more distal elements in the hairpin. In the present study, we have used a reverse genetic strategy, diagrammed in Fig. 1A, to dissect these telomeric sequences and explore the importance of the distal elements.

As shown in Fig. 1B, the unique 121-nucleotide left-end sequence of the negative-sense MVM genome is predicted to fold into a Y-shaped hairpin containing small internal palindromes that form these distal structures, dubbed the hairpin "ears." The 43-bp duplex stem region is interrupted by a mismatched "bubble" sequence, where the triplet 5′-GAA-3′ on the inboard arm of

Received 11 June 2012 **Accepted** 23 August 2012
Published ahead of print 29 August 2012
Address correspondence to Peter Tattersall, peter.tattersall@yale.edu.

doi:10.1128/JVI.01450-12

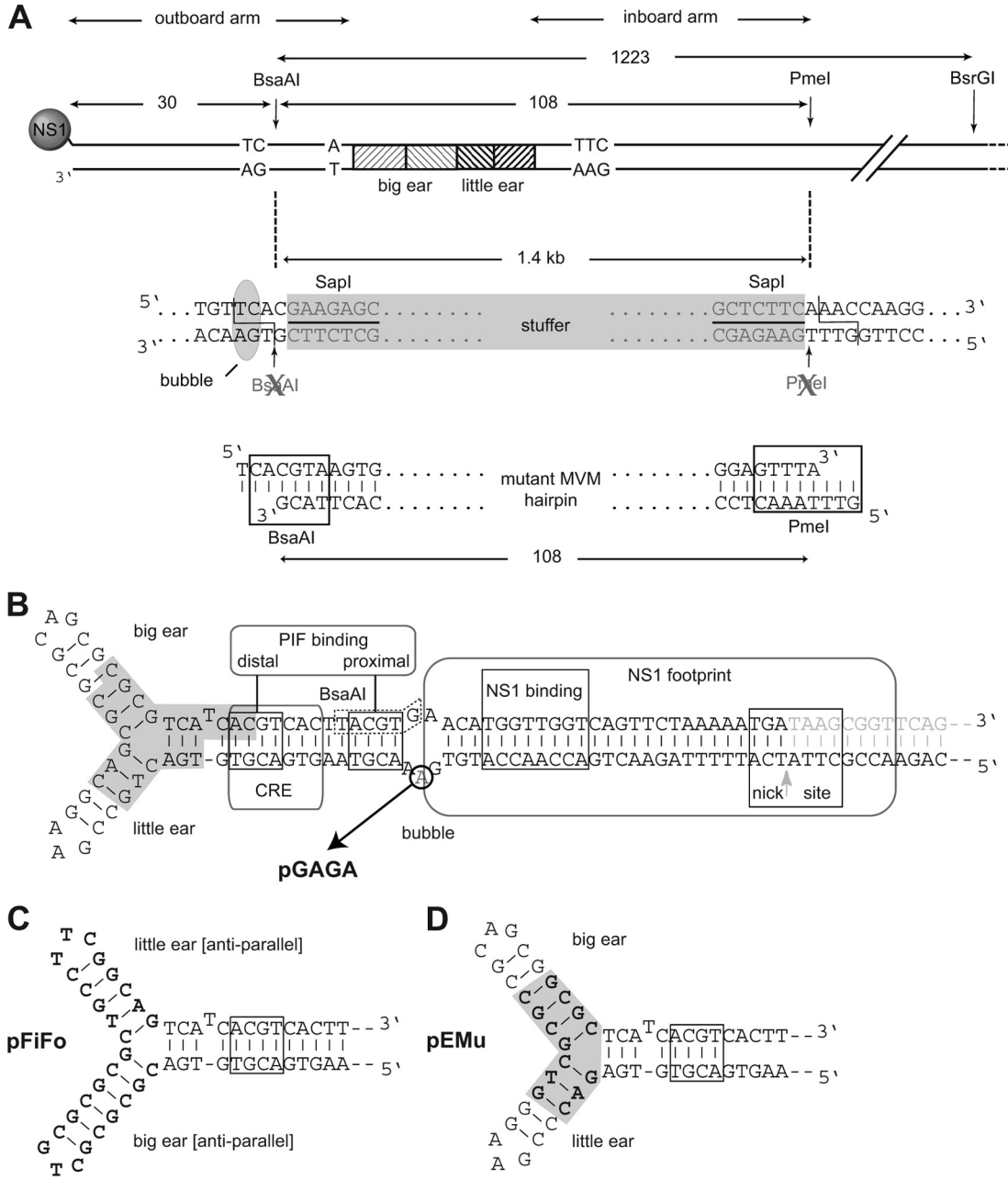

FIG 1 Arrangement of sequences in the extended left-hand end of MVM. (A) Extended left-hand end of monomer RF generated during genomic replication, in which the internal palindromes that form the hairpin ears are represented by hatched rectangles. The locations of the BsaAI, PmeI, and BsrGI sites mentioned in the text are indicated, as is the 1,223-bp BsaAI-to-BsrGI fragment that is captured from infected cell DNA by pCATCH. The middle section diagrams pCLIP-distal, in which a 1.4-kb ϕX174 filler DNA sequence was engineered to include terminal SapI sites, inserted between the BsaAI and PmeI sites. SapI cleaves outside the insert into genomic sequence, allowing the direct insertion of annealed oligonucleotides incorporating the desired mutation(s), as shown in the bottom section. (B) Features of the MVM left hairpin. The shaded region was reported to be protected from hydroxyl radicals by capsid interactions (41). A cellular heterodimer, PIF, binds to spaced proximal and distal 5′-ACGT-3′ half sites. The BsaAI site that overlaps the proximal PIF half site in the duplex form of the outboard strand is indicated by a box with dashed lines. The nucleotide missing in the pGAGA mutant is circled. (C and D) The reorganized sequences (in bold) of the hairpin ears in the pFiFo (C) and pEMu (D) infectious clones.

the hairpin in virion DNA is opposed by the doublet 5′-GA-3′ on the outboard arm. Viral DNA synthesis is initially primed from the 3′ nucleotide of this hairpin, to generate a duplex molecule in which the two strands are linked to one another through the hairpin. However, in contrast to origins that are resolved by terminal resolution, potential origin sequences in the MVM left end cannot be nicked by NS1 in this hairpin configuration. Instead, rolling-hairpin displacement synthesis must proceed so that the hairpin is unfolded and copied to create the fully base-paired palindromic junction spanning adjacent genomes in the dimer RF before the active origin is generated. Within this duplex structure, the sequence from the outboard arm surrounding

the GA bubble dinucleotide creates the active origin, $OriL_{TC}$, while the equivalent sequence from the inboard arm, $OriL_{GAA}$, containing the bubble trinucleotide is inactive. The minimum linear origin sequence is approximately 50 bp in length, extending from two 5′-ACGT-3′ motifs spaced 5 nucleotides apart at one end to a position some 7 bp beyond the nick site (18). The two 5′-ACGT-3′ sequences serve as half sites that cooperatively bind a heterodimeric cellular transcription factor called parvovirus initiation factor (PIF) (13, 14), also known as glucocorticoid modulating element-binding protein (GMEB) (30), which is abundantly expressed in many cell types. The position of the proximal PIF half site relative to the NS1 binding site is absolutely critical for allowing PIF to activate NS1, since the single additional intervening bubble nucleotide of the inboard arm prevents PIF from stabilizing the binding of NS1, which is therefore unable to nick $OriL_{GAA}$ (12).

While the actual sequence of the $OriL_{TC}$ doublet is relatively unimportant, we have shown that insertion of any third nucleotide here inactivates the origin, thus indicating that the bubble is a critical spacer, rather than a recognition element in its own right (18). Subsequently, we reported the use of an oligonucleotide-based reverse genetic approach to disrupt this asymmetry in isolated copies of the viral genome and showed that genomes containing either opposing doublets or triplets in the hairpin bubble did not give rise to plaques (8). However, plaque-forming mutants likely derived from imperfections in the synthetic oligonucleotide pool were isolated at low frequency and were found to contain second-site mutations that restored the asymmetry, either by changing the spacing or by crippling one PIF binding site. These mutations either inactivated an active inboard arm or activated an inactive outboard form of OriL, a polarity that strongly suggested that, at least in the genus *Parvovirus*, an active inboard OriL is highly detrimental to growth. However, this reverse genetic approach did not generate a cloned form of the mutant DNA that could be used to analyze exactly which aspects of the infectious cycle were impaired. In the present study, we use an alternate strategy, diagrammed in Fig. 1A and B, in which the mutation is first cloned into a modified infectious plasmid form of MVM, to reexamine the effects of introducing an active inboard OriL. These studies suggest that gene expression proceeds relatively normally for such viruses but that the DNA amplification mechanism is severely defective.

Although there is remarkable variation in the hairpin telomeres from different genera of the *Parvoviridae* (39), within members of the genus *Parvovirus*, the nucleotide sequence and predicted structure of the left-end hairpin ears are highly conserved, suggesting that they may be involved in essential interactions during the virus life cycle. For example, the junction region between the ears and stem of the hairpin has been reported to interact with the capsid, as indicated in Fig. 1B (40, 41), suggesting that these sequences might potentially mediate important interactions such as the packaging process. We have used the same plasmid-based reverse genetic approach to explore the phenotypes of two mutants in which this conserved sequence arrangement has been disrupted either by inverting the ears, as detailed in Fig. 1C, or by modifying the hairpin branch region by sequence transversion, as shown in Fig. 1D, while conserving its overall nucleotide composition.

MATERIALS AND METHODS

Cells and viruses. The fibrotropic prototype strain of MVM (MVMp; GenBank accession number J02275), derived by transfection of the infectious plasmid clone pdBMVp (31), was grown in monolayer cultures of A9 ouabr11 cells in Dulbecco's modified Eagle's medium (DMEM) containing 5% fetal bovine serum (FBS) and antibiotics.

Mutant plasmids. Infectious clones of MVMp with mutant left-end hairpins were generated using a modified vector, pCLIP-distal, as previously described (35). Briefly, mutation-bearing oligonucleotides were cloned into the recipient vector, which had been predigested with SapI, leaving noncomplementary overhangs within the authentic MVM hairpin sequence that facilitate directional cloning of substitute hairpin sequences. To generate mutant plasmids pGAGA, pFiFo, and pEMu, the following pairs of synthetic oligonucleotides were annealed and ligated into SapI-predigested pClip-distal, and the mixture was transformed into the Sure-2 strain of *Escherichia coli* (Agilent Technologies, Wilmington, DE): for pGAGA the top-strand oligonucleotide is 5′-TCACGTAAGTG ACGTGATGACGCGCGCTGCGCGCGCTGCCTTCGGCAGTCACACGT CACTTACGTTCACATGGTTGGTCAGTTCTAAAAATGATAAGCGG TTCAGGGAGTTTA-3′ and the bottom-strand oligonucleotide is 5′-GT TTAAACTCCCTGAACCGCTTATCATTTTTAGAACTGACCAACCAT GTGAACGTAAGTGACGTGTGACTGCCGAAGGCAGCGCGCGCAG CGCGCGTCATCACGTCACTTACG-3′; for pFiFo, the top-strand oligonucleotide is 5′-TCACGTAAGTGACGTGATGACTGCCGAAGGCAGC GCGCGCAGCGCGCGTCACACGTCACTTACGTTTCACATGGTTGG TCAGTTCTAAAAATGATAAGCGGTTCAGGGAGTTTA-3′ and the bottom-strand oligonucleotide is 5′-GTTTAAACTCCCTGAACCGCTT ATCATTTTTAGAACTGACCAACCATGTGAAACGTAAGTGACGT GTGACGCGCGCTGCGCGCGCTGCCTTCGGCAGTCATCACGTC ACTTACG-3′; and for pEMu, the top-strand oligonucleotide is 5′-TCA CGTAAGTGACGTGATGAGCGCCGCTGCGGCGCGACCCTTCGGG TCTCACACGTCACTTACGTTTCACATGGTTGGTCAGTTCTAAAAAT GATAAGCGGTTCAGGGAGTTTA-3′ and the bottom-strand oligonucleotide is 5′-GTTTAAACTCCCTGAACCGCTTATCATTTTTAGAACTG ACCAACCATGTGAAACGTAAGTGACGTGTGAGACCCGAAGGGT CGCGCCGCAGCGGCGCTCATCACGTCACTTACG-3′.

To overcome problems caused by polymerase slippage when sequencing through complete hairpins, palindromic termini in cloned DNA were digested with BssHII, which cleaves between the hairpin ears, before being subjected to DNA sequencing.

Virus stocks. To generate virus stocks, subconfluent A9 monolayers were transfected with 5 μg of infectious plasmid DNA using Superfect (Qiagen, Valencia, CA) and cultured overnight. On the next day, cells were subcultured 1:4 on 10-cm plates, which were then incubated until they showed cytopathic effects (typically at 72 h). Cells and medium were harvested, and virus was purified on iodixanol gradients as previously described (16) and quantitated on alkaline agarose gels as described below.

Protein expression and Western transfers. A9 cells were seeded as monolayer cultures at 25% confluence and infected with 10,000 viral genomes (vg) per cell. Plates were rocked every 30 min for 4 h, viral inocula were removed, and the cultures were incubated for a further 2 h with fresh medium containing 0.04 units per ml of neuraminidase (*Clostridium perfringens*, type V; Sigma, St. Louis, MO) to remove surface virus, after which the medium was changed once more with medium containing neuraminidase to prevent reinfection. Cells were harvested at 48 h postinfection (p.i.) by scraping, collected by centrifugation in aliquots, resuspended in phosphate-buffered saline containing EDTA-free Complete protease inhibitor cocktail (Roche, Branchburg, NJ), and frozen. Proteins were separated on discontinuous polyacrylamide gels in the presence of sodium dodecyl sulfate (SDS-PAGE), transferred electrophoretically to an Immun-Blot polyvinylidene difluoride membrane (Bio-Rad Laboratories, Hercules, CA), and probed with rabbit antisera as indicated. Blots were developed using horseradish peroxidase-conjugated goat anti-rabbit

IgG, and bands were detected by enhanced chemiluminescence according to standard procedures.

Expansion assays. Productive infection was determined using a virus expansion assay (27). Briefly, A9 cells were seeded onto Teflon-coated spot slides (Cell-Line Associates, Inc., Newfield, NJ) at 20% confluence and infected at 30, 300, or 3,000 vg/cell for 3 h at 37°C. After removal of the inoculum, cells were cultured for 24, 48, or 72 h, before being fixed with 2.5% paraformaldehyde, permeabilized with 0.1% Triton X-100, stained for NS1 by indirect immunofluorescence using the murine monoclonal antibody CE10 (42), and counterstained with DAPI (4′,6-diamidino-2-phenylindole). The percentage of cells with NS1-positive nuclei was scored using a Nikon OptiPhot epifluorescence microscope fitted with a Kodak digital camera driven by MDS 290 software. Multiple images were quantified by single-blinded analysis in Adobe Photoshop.

DNA replication and Southern transfers. Cells were seeded and infected as described for protein expression, including culture in neuraminidase from the point, 2 h p.i., when virus inocula were removed. Typically, cells were harvested at 24 h and 48 h p.i. by scraping into the medium and pelleted by centrifugation, and both cells and medium were stored frozen. Where indicated, cells from a single plate were divided into two equal aliquots to allow differential processing for DNA replication and packaging analysis.

Total viral DNA was analyzed as described previously (21). Where indicated, samples were digested with EcoRI before analysis by electrophoresis through native agarose gels. Two-dimensional (neutral/denaturing) gel analysis was performed as described previously (17). Briefly, samples were first separated by electrophoresis through a native gel; the gel lane was then excised, turned through 90°, and inserted into an extended well, positioned across the top of an alkaline denaturing gel.

For analysis of encapsidated DNA, cell pellets were resuspended in TE8.7 (50 mM Tris-HCl, 0.5 mM EDTA, pH 8.7), and virus was released by 3 cycles of freezing and thawing and clarified by centrifugation. Resulting cell extracts and equivalent samples of culture medium were digested with micrococcal nuclease and analyzed on denaturing agarose gels, as described previously (27).

For Southern blotting, DNA was transferred to Zeta probe membranes (Bio-Rad) according to standard procedures. Blots were generally hybridized with ^{32}P-labeled, random-primed oligonucleotide probes generated using the full MVM genome as the template. To assess strand specificity in the packaging assay, blots were probed with the strand-specific ^{32}P-labeled oligonucleotides NScPOS and NScMIN, which hybridize to positive- and negative-sense DNA between MVM nucleotides 1165 and 1190, respectively (20), and quantitated using a Typhoon Trio variable-mode phosphorimager (GE Healthcare) with ImageQuant software.

Recovery of left-end hairpin sequences from mutant RF. RF DNA of mutant viruses was isolated from infected A9 cells by a modified Hirt procedure (38), and monomer RF was gel purified and digested with BsrGI and BsaAI. The 1,223-bp fragment was further gel purified and cloned into the BsaAI-to-BsrGI backbone fragment of pCATCH, a truncated version of the MVMp infectious clone with a single BsaAI site in the left-end palindrome (35).

Virus competition assays. A9 cells were seeded at 5×10^5 per 60-mm dish and infected with 40 vg/cell of an equimolar mixture of wild-type virus (carrying the variant II probe sequence) and one of the GAGA, FiFo, or EMu mutants (with the standard probe sequence) for 2 h. Cells and medium were harvested after 24 h, 48 h, or 72 h. Cell pellets were resuspended in 0.2 ml TE8.7, virus release was by freezing and thawing (3 times), and extracts were clarified by centrifugation, before storage at −20°C. For analysis, cell-equivalent amounts of cell extract and culture medium were pooled and digested with micrococcal nuclease to remove all nonpackaged DNA, the reaction was stopped with EGTA, and standard and variant genome concentrations were assayed over a range of dilutions by differential quantitative PCR (qPCR).

Differential real-time qPCR. The multiplex TaqMan reverse transcription-qPCR assay was described previously (35). Briefly, the variant II wild-type virus incorporates silent mutations that allow it to bind the fluorescent probe 5′-VIC-TAGGTTCCAGTAGCGAACTCATCGCCA-TAMRA-3′ (where TAMRA is 6-carboxytetramethylrhodamine), while each of the standard viruses binds the fluorescent probe 5′-FAM-TAAGTGCCTGTGGCAAATTCGTCCCCT-TAMRA-3′ (where FAM is 6-carboxyfluorescein). PCR amplification was accomplished with primers GF-UP-TAQ (5′-CACAACAAATCACATTGCTCAGAA-3′) and GF-DOWN-TAQ (5′-TTGCCACGTGTGTGTGAGTTT-3′). Samples were analyzed using an Applied Biosystems Prism 7700 sequence detection system instrument and software.

RESULTS

The three mutants are viable but show different levels of fitness. Since parvoviral terminal palindromes are difficult to manipulate, we have developed a method for the directional cloning of synthetic oligonucleotides carrying left-end mutations directly into a deletion plasmid form of the viral sequence, such that they reconstitute the left-end terminal palindrome of the infectious genome (35), as described in the Materials and Methods section. Using this approach, we reassessed the effects of removing a single nucleotide from the bubble asymmetry in the inboard arm of the left-end hairpin, generating a mutant plasmid, pGAGA (opposing GA doublets; Fig. 1B), which should be nicked on both sides of the palindromic junction sequence present in dimer RF. Similarly, the significance of the asymmetric ears of this hairpin was probed using two mutants: pFiFo (Flip stem with Flop ears; Fig. 1C), in which the stem of the hairpin remains in its original Flip orientation but the ears are inverted, and pEMu (ears mutated), in which the nucleotide composition of the putative capsid-binding domain at the base of the ears is conserved but its sequence is replaced by a series of transversions (Fig. 1D).

After confirming their DNA sequences, mutant plasmids were transfected into subconfluent monolayers of A9 cells, which were then cultured for several days until they showed cytopathic effects (CPEs). In cells transfected with wild type and the two hairpin ear mutant plasmids pFiFo and pEMu, CPE was apparent at between 72 and 96 h posttransfection and rapidly led to extensive cell lysis. By 120 h, we also observed CPE in cells transfected with the hairpin stem mutant pGAGA, indicating that this mutant is viable, albeit substantially impaired relative to wild type. This was unexpected, since we had previously shown that a similar mutant, constructed as a ligated synthetic hairpin molecule, was unable to generate plaques following transfection (8).

Full virus particles containing the viral genome were extracted from cells transfected with each mutant plasmid and purified by sedimentation to equilibrium in iodixanol step gradients, and viral genomes were quantified by denaturing gel electrophoresis and Southern transfer (27). The ability of these virion stocks to support the expression of each of the viral proteins in a single round of infection was then examined. As shown in Fig. 2A, each mutant was able to express all of the viral proteins (NS1, NS2, VP1, and VP2), but whereas FiFo achieved protein levels that were similar to those of wild type at this time and input multiplicity, viruses bearing the EMu and GAGA mutations were somewhat impaired (2- to 4-fold) for expression of each protein.

We then examined the kinetics of viral spread in cultures infected at input multiplicities of 3,000, 300, or 30 vg/cell. About 60% of the cells receiving 3,000 vg/cell of wild-type virus expressed nuclear NS1 by 48 h p.i. (Fig. 2B). In contrast, at this time point, ~40% of cells infected with the FiFo mutant and only 10 to 20% of cells infected with the EMu or GAGA viruses were NS1 positive.

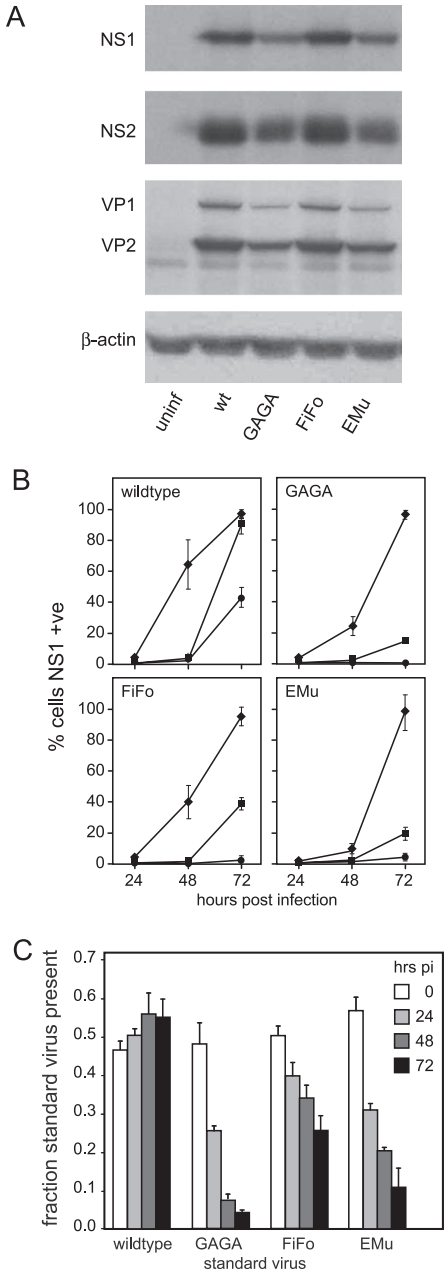

FIG 2 Comparison of mutant infection parameters with those of wild-type virus. (A) Western blot analysis of intracellular viral protein expression at 48 h p.i. Viral proteins were detected using polyclonal antibodies against the common amino terminus of the nonstructural proteins NS1 and NS2 (top and upper middle), and the structural proteins VP1 and VP2 were detected with polyclonal antibodies against denatured capsid protein (lower middle). Reactivity to antibody against β-actin was used as a loading control (bottom). uninf, uninfected; wt, wild type. (B) Viral expansion kinetics in multiple-round, single virus infections of A9 cells at 3,000 (◆), 300 (■), or 30 (●) vg/cell of wild type or each of the three mutants, measured by NS1 expression. (C) Fitness of each mutant relative to wild type, determined by differential qPCR in multiple-round coinfections of A9 cells with matched input multiplicities (40 vg/cell) of standard mutant and variant wild-type virions harvested at the indicated times p.i.

Thus, while viable, the mutants showed variably impaired overall fitness relative to the wild-type virus. By 72 h p.i. at this input multiplicity, all infections had progressed and essentially all cells were NS1 positive. In contrast, by 72 h at lower input multiplicities, wild-type virus gave 80% NS1-positive cells at 300 vg/cell and 40% at 30 vg/cell, while the level of infection supported by each mutant was substantially impaired, so that it remained minimal at 30 vg/cell and affected only a subpopulation of cells at 300 vg/cell (~40% for FiFo, 20% for EMu, and <10% for GAGA). Thus, while inversion of the hairpin ears in the FiFo mutant did not prevent progeny virion production, it did have a marked effect on the efficiency with which it spread through the culture, while simple sequence transversion at the base of both ears had a much more pronounced effect on viral fitness. Similarly, deleting a single nucleotide from the bubble sequence on the inboard arm of the left-end palindrome in the GAGA mutant had a profoundly negative effect on viral fitness but did allow some virus expansion.

To verify these differences under optimally matched culture conditions, pairwise coinfections of wild type and each mutant were assayed using differential quantitative PCR, as described previously (35). For this assay, a wild-type virus marked with a series of synonymous mutations in the coat protein gene was paired with each hairpin mutant in matched, low-multiplicity coinfections that were allowed to develop over several cycles of infection, so that exactly the same conditions held for both viruses. At 24-h intervals, progeny virus from each coinfection was quantified by PCR, using differentially tagged probes that distinguished between the two initiating genomes. As seen in Fig. 2C, in control cells coinfected with a mix of variant and standard wild-type viruses, the ratio of the initiating genomes remained relatively constant over time. However, when each of the three mutant viruses was mixed with wild-type virus, the mutants proved variably defective. While FiFo and EMu were reduced by 2- and 5-fold, respectively, over the 72 h of coinfection, GAGA was reduced by more than 10-fold over the same period, indicating that this mutant was significantly more impaired than the other two.

The hairpin ear mutants are stable, whereas the stem mutant is not. Since we had previously found that the mutation in pGAGA abrogated plaque formation and we expected the sequence rearrangements introduced into the left-end hairpin of pFiFo and pEMu to affect viability more drastically than observed, we considered the possibility that the mutant genomes had rapidly acquired compensating mutations or had reverted to wild type as a consequence of the junction resolution reaction. To test for either of these possibilities, we used a plasmid capture system, pCATCH, to isolate the left-end sequences of individual monomer RF molecules, as described in Materials and Methods. As seen in Fig. 3A, all of the left-end termini isolated from FiFo- or EMu-infected cells maintained the mutant sequence, indicating that these mutant forms of the terminus could support replication and that the phenotypes observed in these infections were due to behavior intrinsic to each mutant. However, the result obtained for the GAGA mutant was quite different. We had great difficulty in obtaining clones from GAGA monomer RF isolated at 24 h p.i., but the two that we were able to isolate and sequence were identical to the mutant. We then isolated DNA from infected cells at 48 h and obtained a further 12 clones, whose left-end sequences are summarized in Fig. 3B. Of these, only three maintained the original GAGA left-end terminal sequence and thus retained the active mutant inboard (GA) origin. One clone (clone 6) had an A inserted into the inboard bubble, thus restoring the inactive wild-type sequence, and the remaining eight had sustained single nucleotide substitutions. Notably, these substitutions always occurred in the vicinity of the bubble sequence, and six clones with

A

pCATCH	GAGA	FiFo	EMu
sequenced clones	14	14	8
same as input	5	14	8
mutant to wildtype	1	0	0
other changes	8	0	0

B

wildtype

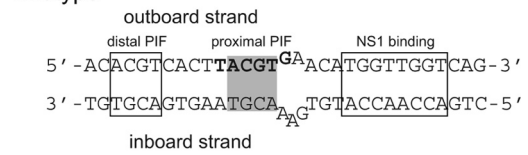

pGAGA:

pCatch GAGA:

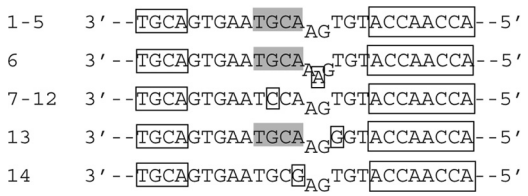

FIG 3 Isolation and characterization of revertants. (A) Total numbers of sequenced pCATCH clones isolated from duplex viral RF DNA, characterized as unchanged clones, revertants, or second-site revertants; (B) catalog of sequences for the 14 left-end clones isolated from GAGA mutant virus-infected cells, as described in the text.

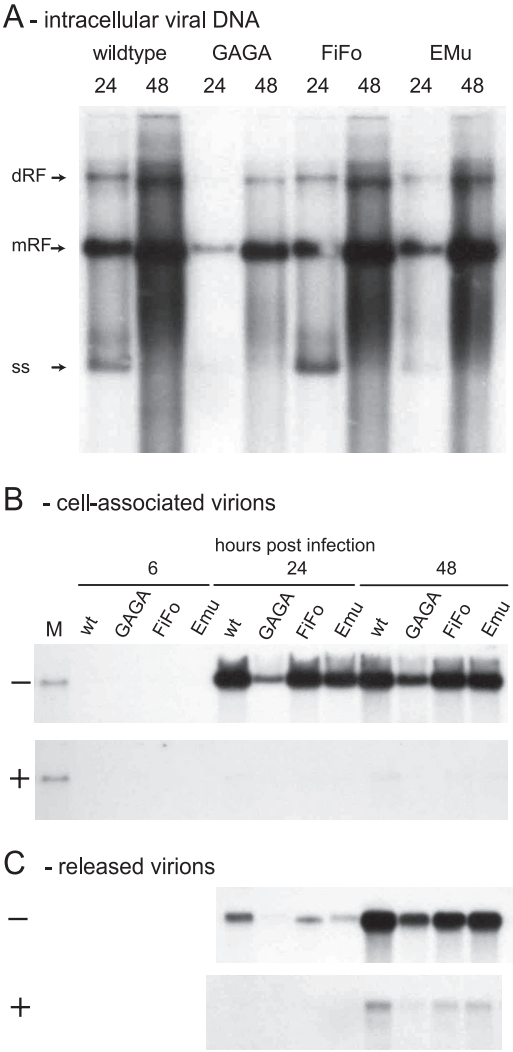

FIG 4 Analysis of mutant and wild-type viral DNA replication and packaging. (A) Agarose gel and Southern blot analysis of total viral DNA extracted from cells at 24 and 48 h p.i. with 10,000 vg/cell input under single-cycle infection conditions. Migration positions of dimer RF (dRF), monomer RF (mRF), and progeny single strands (ss) are indicated. (B and C) Equivalent aliquots of cell extract (B) and culture medium (C) were digested sequentially with micrococcal nuclease and proteinase K, as described in Materials and Methods, and then electrophoresed through an alkaline agarose gel, blotted, and probed with labeled oligonucleotides specific for the negative (−) or positive (+) strands. Lane M, control duplex DNA marker.

the single nucleotide mutations (Fig. 3B, clones 7 to 12) substituted a C for the G of the invariant CpG central dinucleotide of the proximal PIF/GMEB binding half site. Such mutations eliminate PIF binding to this site (7, 14) and thus would block establishment of the NS1 nicking complex on the inboard arm and effectively inactivate the engineered inboard origin. Of the remaining two second-site mutants, one (clone 13) substitutes a G for the T immediately beyond the bubble, while the other (clone 14) substitutes a G for the A in the proximal PIF ACGT half site. Both of these mutations therefore increase the size of the bubble in the hairpin stem and change the G+C content of the nicking template, while the latter also impairs PIF binding to the critical NS1-proximal half site. Accordingly, the single true revertant and all of the second-site mutations would be expected to suppress the activity of the mutant inboard origin, effectively reverting the replication phenotype of the GAGA mutation. Importantly, since the recovered sequences modify only the inboard arm, the observed changes would not be expected to impair normal viral DNA replication.

Mutation of the hairpin stem, but not its ears, negatively affects viral DNA replication and packaging. Next we examined the types and quantities of replication intermediates produced by each virus in high-multiplicity single-round infections. As seen in Fig. 4A, both monomer and dimer RF DNA accumulated to similar levels in wild-type, FiFo, and EMu infections by 24 or 48 h p.i. However, there was a profound deficiency in RF accumulation in cells infected with the GAGA mutant, so that it was minimal at 24 h, while by 48 h it approximated the level seen at 24 h with the other viruses. Since the GAGA mutant initiated infection and expressed all viral proteins with reasonable efficiency (Fig. 2A), it therefore appears likely that its primary defect involves replication initiation or the DNA amplification mechanism.

While both wild type and FiFo also accumulated significant levels of intracellular progeny single-stranded DNA by 24 h, as seen in Fig. 4A, this had diminished by 48 h, at least in part due to virus release (see below), while the levels for EMu always appeared to be lower and GAGA was undetectable. However, total DNA extraction followed by native agarose gel electrophoresis is a suboptimal method for quantifying single-stranded DNA because the

released single strands undergo variable intra- and intermolecular annealing with other partially single-stranded DNAs in the mixture and, rather than reliably migrating as denatured single strands, run as a smear down the gel, ending at the position of the denatured strands. To determine packaging efficiency under more rigorous conditions, a nuclease protection packaging assay (27) was used in which infected cell extracts were digested with micrococcal nuclease to remove unprotected DNA, the enzyme was inactivated, and virion DNA was extracted and analyzed by electrophoresis through denaturing alkaline gels. Packaged DNA was quantified by Southern blotting using two different, strand-specific probes, as described in Materials and Methods. Single-round infections were carried out in the presence of neuraminidase, which prevents progeny virions from initiating a second round of infection, and samples from the final culture medium were included in the packaging assay to analyze virus released from the cell during infection. The results of such an analysis are shown in Fig. 4B and C. No packaged input virus was seen at 6 h p.i. for any of the viruses, and at 24 h, the great majority of packaged viral DNA was found in the intracellular fraction (Fig. 4B), while by 48 h, approximately 50% of the total virions had been released from the cell (Fig. 4C). Accumulation of packaged DNA by the EMu mutant appeared to be slightly retarded compared to that by either FiFo or wild type, while intracellular levels suggested that packaging of GAGA single-stranded DNA was conspicuously restricted. However, GAGA virions were released from the cell with normal kinetics, so that by 48 h equal accumulations were present in cells and medium. When added together, total packaged GAGA DNA at 48 h did approximately correspond to the defect in RF accumulation discussed previously. We conclude that none of the mutants have a substantial packaging defect *per se* and, similarly, that none of them exhibit a conspicuous virion-release defect. Importantly, at all time points and for both intracellular and extracellular virus, all three mutants paralleled the wild type in packaging predominantly the negative-sense strand, such that any trace of packaged plus strand was observed only at the highest levels of viral DNA input per gel lane. Since strand selection reflects the relative efficiency at which left- and right-end genomic termini are resolved (20), this indicates that merely activating a second nick site in the duplex GAGA dimer junction sequence failed to enhance the resolution efficiency of this telomere.

In order to explore the underlying defect(s) in mutant viral DNA replication, especially for the GAGA mutant, the RF pool DNA was extracted from infected cells at 48 h p.i. and digested with EcoRI, which cuts the predominantly monomeric duplex RF twice. The left and right termini of monomer RF molecules exist in two conformations, either as a covalently closed turnaround form, in which both strands of the genome are linked through the hairpin, or as an extended form, containing an open-ended duplex copy of the entire terminal palindrome (23), as diagrammed in Fig. 5A. Thus, EcoRI digestion yields one homogeneous internal fragment and two terminal fragments that each exist in two forms, which can be separated on neutral agarose gels to give the doublets shown in Fig. 5B. Despite the previously discussed differences in overall DNA synthesis observed for these four viruses, the patterns of turnaround versus extended forms of the right-end telomere were very similar at both time points, although at 24 h, GAGA forms were difficult to see and required a longer exposure (Fig. 5B). Specifically, at 24 h, extended forms of the right end vastly predominated, while by 48 h, turnaround forms had begun to

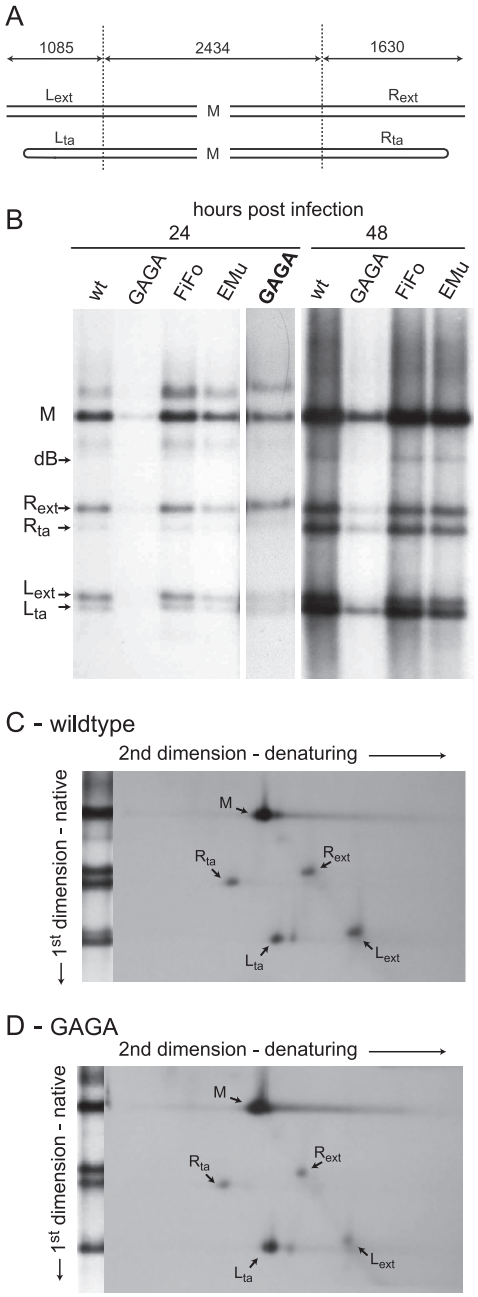

FIG 5 Analysis of left- and right-end forms of replicating wild-type and mutant DNA. (A) Cartoon depicting the structures of the two forms of each end, as previously determined (23). (B) Total DNA from single-cycle infections was digested with EcoRI, electrophoresed through a neutral agarose gel, and then blotted and probed as described in Materials and Methods. The lane indicated by boldface GAGA is a long exposure of a DNA sample extracted from GAGA-infected cells at 24 h p.i. (C and D) Two-dimensional agarose gel electrophoresis of total DNA extracted from wild-type (C) and GAGA (D) virus-infected cells. DNA was first run in a nondenaturing neutral gel, turned through 90°, and run into a denaturing alkaline gel, followed by transfer and probing as described in Materials and Methods. M, middle fragment; L_{ext}, left extended form; R_{ext}, right extended form; dB, dimer bridge; R_{ta}, right turnaround; L_{ta}, left turnaround.

accumulate and constituted about 50% of the total termini. While a similar situation prevailed for the left-end fragments of wild type, FiFo, and EMu at these two time points, by 24 h, the left-end terminus of GAGA was represented by approximately equal num-

bers of extended and turnaround forms, while by 48 h, the larger extended forms were almost absent and the single dominant form comigrated with the turnaround fragment of other viruses.

To confirm that the observed GAGA left-end fragment did represent a terminus in the turnaround configuration, we compared wild-type and GAGA EcoRI digests by two-dimensional (2D) electrophoresis (17), during which fragments separated in the neutral dimension are rotated 90° and reelectrophoresed under denaturing conditions. For wild-type DNA, shown in Fig. 5C, this resulted in clear separation of the left-end extended form, L_{ext}, which migrated with the same molecular length in both dimensions, and the left-end turnaround form, L_{ta}, which migrated in the alkaline dimension at a position indicating that it was twice the length that it displayed in the neutral gel. In support of the interpretation that the GAGA mutant accumulated RF with predominantly left-end turnaround termini, Fig. 5D shows that the double-length form, L_{ta}, comprised the bulk of the signal in the 2D gel for this terminus, in contrast to the approximately equal distribution between the two forms shown in Fig. 5C for wild-type virus. Thus, a mutation that *in vitro* effectively activates the nick site derived from the inboard arm of the hairpin (data not shown) and that might thus be expected to double the rate at which extended forms were generated in fact suppressed its formation throughout infection, drastically curtailing RF amplification. This suggests that duplex junction resolution involves an additional mechanistic constraint that is not fully envisaged in the current heterocruciform resolution model (25).

Since packaged GAGA DNA was released from infected cells, it is likely that most of the GAGA extended forms generated by the 48-h time point had already been released as progeny virus. Remaining RF DNA existed as a covalent duplex, which appeared to be increasingly difficult to resolve as the infection proceeded, making the culture susceptible to hijack by mutants that did not share the GAGA defect, as observed (Fig. 3). The pCATCH technique used here to capture termini can sample telomeres only in the extended configuration, which presumably explains why the GAGA fragment was difficult to clone from DNA extracted at 24 h p.i. and why that obtained at 48 h predominantly contained second-site mutations.

DISCUSSION

Roles(s) of structure versus sequence in the hairpin ears. In this study, we show that the Flip sequence orientation of the hairpin ears at the left end of the MVM genome is not absolutely required for any step in the viral life cycle, even though this orientation is strictly conserved by the viral replication mechanism. Since the MVM genome is packaged in a 3′-to-5′ direction (19), it is highly likely that the left-end hairpin is in some way involved in the early stages of packaging. However, we found little evidence for any sequence or orientation specificity in the packaging efficiency of the FiFo and EMu mutants. Instead, recovery of virions following transfection of these mutant plasmids corresponded approximately to that of wild type both in kinetics and in yield, and infection with the resulting virions gave rise to approximately equivalent levels of viral duplex RF DNA, although such viruses were somewhat less fit than wild type when used to coinfect the same cell population or when allowed to expand through multiple rounds of infection. This indicates that while the wild-type sequence may be preferred, this sequence is not required to be specific, which thus suggests that it may be the terminal DNA structure, rather than its sequence, that is critical. This finding parallels early observations with adeno-associated virus type 2 (AAV2), where terminal substitutions that maintained the forked nature of the ITR were tolerated, suggesting that structure was more important than sequence (5). However, at present, precise structural information is not available for any parvoviral termini. *In silico* polynucleotide folding generates various 2D arrangements of the wild-type, FiFo, and EMu hairpins that are closely related to those presented in Fig. 1. These are characterized by relatively small differences in ΔG, suggesting that the structure of the terminus might be quite flexible and could therefore be trapped in particular 3D configurations *in vivo* by specific physical interactions. If so, then the transversions present in EMu or the sequence rearrangement present in FiFo does not radically alter its potential to form such a structure, since, as shown in Fig. 2C, we observed that both mutants are almost as fit as wild type.

Whether or not the tertiary structure of the terminal hairpin mediates specific interactions with the capsid, it is not yet clear when this binding might occur and for what step in the viral life cycle it might be required. Since packaging occurs in the 3′-to-5′ direction, one possibility would be that such an interaction locks the 3′ end of progeny strands onto the capsid as a first step in the encapsidation process. This idea fits with the fact that the 3′ end of each strand of AAV2, in which both strands are packaged, would be predicted to form the same structure, since these viruses are homotelomeric. This model would also fit with the predominantly negative-strand encapsidation seen for members of the genus *Parvovirus*, for which the 3′ end of the packaged strand comprises the unique Flip sequence of the left-end hairpin. However, there are exceptions to the negative-strand packaging rule in this heterotelomeric genus, such as the virus LuIII, which encapsidates both strands (4), even though the structure of the 3′ hairpin of the positive strand is predicted to be quite different from that of the negative strand. Significantly, a single base insertion in the OriR sequence of MVM leads to the displacement of approximately equal numbers of each strand and both strands are encapsidated with similar efficiencies (20), making it hard to envisage how such a left-end packaging interaction might function.

An alternative role for docking the left-end hairpin with the capsid might be to anchor the newly uncoated genome to its particle at the start of infection, since uncoating also proceeds in a 3′-to-5′ direction (16, 22). This model suggests that the capsid might be involved in targeting the genome to a specific nuclear site or subcompartment and that association of the newly emerged duplex template with the capsid might be necessary to anchor it in a location favorable for its active transcription. Such a model would imply that MVM particles containing aberrantly packaged positive strands and MVM genomes with structurally defective left-end hairpins would have a significantly lower infectivity than their normal counterparts. In support of this idea, we have recently been able to package MVM genomes with single-ear hairpins and find that they enter cells normally but are unable to initiate nonstructural gene expression (L. Li, S. F. Cotmore, and P. Tattersall, unpublished data).

A second active OriL perturbs junction resolution and is rapidly lost *in vivo*. In contrast to the ear mutations, removing the asymmetry in the stem sequence that controls asymmetric resolution of this palindrome did prove highly deleterious. The wild-type left end is arranged so that a potential inboard origin sequence is inactive due to the presence of an additional nucleotide

within a spacer region, dubbed the bubble, and in a previous study, we had been unable to generate infectious foci from genomes with mutations that activated this origin (8). While we originally concluded that such mutants were nonviable, the results presented here for the GAGA mutant, obtained using a reverse genetic technique that allows construction of mutants with hairpin mutations in plasmid form, reveal that this mutant can, in fact, be recovered as a burst of packaged, infectious virus that carries the original mutation. However, it appears that having two active origins is so deleterious to virus growth that the original mutant is rapidly supplanted by mutants with second-site mutations in which the function of the inboard origin is disrupted. This was achieved either by restoring the additional inserted nucleotide, by disrupting the duplex across the bubble, or by mutating the Pu CGPy sequence of the bubble-proximal half site for binding PIF/GMEB. This conclusion is consistent with the polarity observed in our previous analysis, in which second-site mutations restored viral viability either by inactivating the second active inboard origin or, for mutants in which both origins were defective, by reactivating the mutated outboard origin (8).

Sequential left-end cloning from GAGA-infected cells also indicated that second-site mutations accumulated as a function of viral expansion. That this was occurring within a few cycles of infection is not unexpected, since mutation rates seen for the parvoviruses are equivalent to those seen for RNA viruses rather than those seen for the more genetically stable double-stranded DNA viruses (34). However, our ability to isolate intact replicating GAGA genomes from early rounds of infection showed that the rate of appearance of compensating mutations was low enough that meaningful short-term experiments could be performed with stocks derived by mass transfection. These revealed that viral gene expression proceeds relatively normally in cells infected with the GAGA mutant, despite the severe limitations in the accumulation of potential duplex DNA templates.

Thus, the GAGA mutation is not lethal because the assembly or activity of nicking complexes on the inboard arm of the hairpin competes with or otherwise disrupts binding of upstream control elements essential for activation of the P4 promoter (26, 36), thus suppressing early viral transcription, as previously hypothesized (8). Rather, the GAGA mutant appears to be profoundly impaired in its ability to synthesize extended forms of the left-hand end of the genome, whereas wild-type junction resolution generates a distinct 50:50 ratio of extended and turnaround termini, both *in vitro* and *in vivo* (17, 21). This result is somewhat counterintuitive, since one might predict that the ability to nick simultaneously on both sides of the dimer junction would allow subsequent synthesis to resolve the junction by producing extended versions of both resulting termini. However, the current model for left-end junction resolution is based on evidence for a heterocruciform intermediate (25) and for its resolution by a mechanism that initiates with the melting and hairpin rearrangement of the extended duplex arm of this cruciform, allowing the 3′ nucleotide to prime synthesis back along its parental negative-sense strand and thus create a telomere in the turnaround configuration. Since the inboard origin in wild-type junctions cannot be nicked, the residual duplex structure is then believed to await resolution by a rate-limiting mechanism, which we have suggested may involve the periodic melting of the inboard nick site, followed by single-strand cleavage, although compelling experimental evidence for this final step remains elusive. The present data suggest that creating a second active origin in the junction may not totally disrupt the heterocruciform resolution mechanism early in infection, since the ratio of extended to turnaround left ends appears to be normal. However, the process goes awry later in infection, perhaps because attempting to form initiation complexes simultaneously at both active origins in the same junction is detrimental to the resolution process, and the frequency with which this occurs escalates as the intranuclear concentration of NS1 molecules increases later in infection. Further studies will be needed to probe the mechanism underlying this defect, but the initial observation does suggest that dimer resolution is a complex and necessary process that cannot be short-circuited by providing two active origins at the left end.

Despite the mutation's negative effect on DNA amplification and progeny production, we were able to obtain packaged minus-strand mutant genomes from cells transfected with the cloned form of GAGA. These maintained their mutant left end through at least a few rounds of replication; thus, it would appear that the mechanism producing turnaround left ends from GAGA cannot be absolute. The fact that we could clone intact mutant GAGA left ends using the pCATCH approach supports the conclusion that these extended forms are produced from mutant copies of the viral DNA and not from emerging revertant genomes.

Influence of asymmetric junction resolution on the hairpin ears. While a significant diversity of terminal hairpin sizes and predicted structures exists across the family *Parvoviridae*, these properties are remarkably conserved within individual genera, despite the fact that the phylogenetic clustering of parvoviral species uses coding sequences and ignores those nucleotides that constitute the terminal palindromes (39). Likewise, all of the members of each genus are either homo- or heterotelomeric, a property that appears to have profound consequences for the genetic strategy and natural history of each genus. Taken with the observation that the terminal sequences are under evolutionary selection to remain conserved during speciation within the genus itself, this suggests that the hairpins play an important role or roles in establishing and maintaining the differences in lifestyle adopted by each genus.

While these roles mostly remain enigmatic, there is at least one well-characterized function ascribed to the hairpin ears in a member of the genus *Dependovirus*. Early methylation interference and nuclease protection studies showed that proteins isolated from infected cells make contact with one of the ears of the AAV2 ITR (1, 29). This interaction was shown to occur between the major replicator protein Rep68/72 and a sequence of five bases, called the Rep binding element′ (RBE′), located at the tip of one of the hairpin ears (37). In the absence of the RBE′, origin firing by Rep is quite inefficient and cannot be enhanced by providing the RBE′ in *trans* (11). The *cis*-acting nature of this interaction has led to the suggestion that it alters the structural stability of the Rep-Ori complex (28), perhaps by rendering the cleavage site single stranded (6).

In contrast, the OriL of MVM is highly active as an isolated 60-bp duplex sequence embedded in a circular plasmid in the complete absence of hairpin ear sequence elements (18), and the stabilization and activation of the MVM NS1 nickase at OriL are achieved by formation of a precise ternary complex with the host factor PIF/GMEB (12). Likewise, although efficient replication of the AAV2 genome requires the Rep-RBE′ interaction, this requirement cannot be absolute, since Rep also cleaves AAVS1, its

recognition site for integration on human chromosome 19, in the absence of any adjacent RBE′-like sequence (32, 33).

While the results presented here do not define a particular role for the hairpin ears or for the maintenance of the Flip orientation in the wild-type genome, they do underscore properties of the parvovirus genome for which they are not responsible. On one hand, neither the orientation nor the sequences of the ears contribute to the negative-strand selection process employed by members of the genus *Parvovirus*. Indeed, our finding that such progeny genomes as the GAGA mutant genome is able to package are as predominantly negative strand as the wild type indicates that the asymmetry of dimer junction resolution plays no role in strand sense selection.

On the other hand, our results show that although the wild-type version of the left-end hairpin is observably preferred in head-to-head competition, the Flip orientation and specific sequence of the left-end ears are by no means essential for viral viability. Since disruption of the arrangement of active and inactive origins in the hairpin stem is so strongly selected against, we can conclude that the asymmetry of dimer junction resolution is critical for some aspect of the viral life cycle and that conserving the Flip orientation of the hairpin ears is merely a consequence of this mechanism rather than its *raison d'être*.

ACKNOWLEDGMENTS

Oligonucleotides used in this project were synthesized in the HHMI Biopolymer Laboratory and W. M. Keck Foundation Biotechnology Resource Laboratory at Yale University.

This work was supported by Public Health Service grant AI026109 from the National Institute of Allergy and Infectious Diseases.

REFERENCES

1. **Ashktorab H, Srivastava A.** 1989. Identification of nuclear proteins that specifically interact with adeno-associated virus type 2 inverted terminal repeat hairpin DNA. J. Virol. **63**:3034–3039.
2. **Astell CR, Smith M, Chow MB, Ward DC.** 1979. Structure of the 3′ hairpin termini of four rodent parvovirus genomes: nucleotide sequence homology at origins of DNA replication. Cell **17**:691–703.
3. **Astell CR, Thomson M, Chow MB, Ward DC.** 1983. Structure and replication of minute virus of mice DNA. Cold Spring Harbor Symp. Quant. Biol. **47**(Pt 2):751–762.
4. **Bates RC, Snyder CE, Banerjee PT, Mitra S.** 1984. Autonomous parvovirus LuIII encapsidates equal amounts of plus and minus DNA strands. J. Virol. **49**:319–324.
5. **Bohenzky RA, LeFebvre RB, Berns KI.** 1988. Sequence and symmetry requirements within the internal palindromic sequences of the adeno-associated virus terminal repeat. Virology **166**:316–327.
6. **Brister JR, Muzyczka N.** 2000. Mechanism of Rep-mediated adeno-associated virus origin nicking. J. Virol. **74**:7762–7771.
7. **Burnett E, Christensen J, Tattersall P.** 2001. A consensus DNA recognition motif for two KDWK transcription factors identifies flexible-length, CpG-methylation sensitive cognate binding sites in the majority of human promoters. J. Mol. Biol. **314**:1029–1039.
8. **Burnett E, Cotmore SF, Tattersall P.** 2006. Segregation of a single outboard left-end origin is essential for the viability of parvovirus minute virus of mice. J. Virol. **80**:10879–10883.
9. **Burnett E, Tattersall P.** 2003. Reverse genetic system for the analysis of parvovirus telomeres reveals interactions between transcription factor binding sites in the hairpin stem. J. Virol. **77**:8650–8660.
10. **Burnett ED.** 2002. Genetic and functional analysis of a parvoviral hairpin telomere. PhD thesis. Yale University, New Haven, CT.
11. **Chiorini JA, et al.** 1994. Sequence requirements for stable binding and function of Rep68 on the adeno-associated virus type 2 inverted terminal repeats. J. Virol. **68**:7448–7457.
12. **Christensen J, Cotmore SF, Tattersall P.** 2001. Minute virus of mice initiator protein NS1 and a host KDWK family transcription factor must form a precise ternary complex with origin DNA for nicking to occur. J. Virol. **75**:7009–7017.
13. **Christensen J, Cotmore SF, Tattersall P.** 1997. A novel cellular site-specific DNA-binding protein cooperates with the viral NS1 polypeptide to initiate parvovirus DNA replication. J. Virol. **71**:1405–1416.
14. **Christensen J, Cotmore SF, Tattersall P.** 1997. Parvovirus initiation factor PIF: a novel human DNA-binding factor which coordinately recognizes two ACGT motifs. J. Virol. **71**:5733–5741.
15. **Cotmore S, Tattersall P.** 2006. Genome structure and organisation, p 74–94. *In* Kerr J, Cotmore S, Bloom M, Linden R, Parrish C (ed), The parvoviruses. Hodder Arnold, London, United Kingdom.
16. **Cotmore SF, Hafenstein S, Tattersall P.** 2010. Depletion of virion-associated divalent cations induces parvovirus minute virus of mice to eject its genome in a 3′-to-5′ direction from an otherwise intact viral particle. J. Virol. **84**:1945–1956.
17. **Cotmore SF, Nuesch JPF, Tattersall P.** 1993. Asymmetric resolution of a parvovirus palindrome in vitro. J. Virol. **67**:1579–1589.
18. **Cotmore SF, Tattersall P.** 1994. An asymmetric nucleotide in the parvoviral 3′ hairpin directs segregation of a single active origin of DNA replication. EMBO J. **13**:4145–4152.
19. **Cotmore SF, Tattersall P.** 2005. Encapsidation of minute virus of mice DNA: aspects of the translocation mechanism revealed by the structure of partially packaged genomes. Virology **336**:100–112.
20. **Cotmore SF, Tattersall P.** 2005. Genome packaging sense is controlled by the efficiency of the nick site in the right-end replication origin of parvoviruses minute virus of mice and LuIII. J. Virol. **79**:2287–2300.
21. **Cotmore SF, Tattersall P.** 1992. In vivo resolution of circular plasmids containing concatemer junction fragments from minute virus of mice DNA and their subsequent replication as linear molecules. J. Virol. **66**: 420–431.
22. **Cotmore SF, Tattersall P.** 2012. Mutations at the base of the icosahedral five-fold cylinders of minute virus of mice induce 3′-to-5′ genome uncoating and critically impair entry functions. J. Virol. **86**:69–80.
23. **Cotmore SF, Tattersall P.** 1988. The NS-1 polypeptide of minute virus of mice is covalently attached to the 5′ termini of duplex replicative-form DNA and progeny single strands. J. Virol. **62**:851–860.
24. **Cotmore SF, Tattersall P.** 2006. Parvoviruses, p 593–608. *In* DePamphilis M (ed), DNA replication and human disease. Cold Spring Harbor Laboratory Press, Cold Spring Harbor, NY.
25. **Cotmore SF, Tattersall P.** 2003. Resolution of parvovirus dimer junctions proceeds through a novel heterocruciform intermediate. J. Virol. **77**: 6245–6254.
26. **Faisst SR, Perros M, Deleu L, Spruyt N, Rommelaere J.** 1994. Mapping of upstream regulatory elements in the P4 promoter of parvovirus minute virus of mice. Virology **202**:466–470.
27. **Farr GA, Tattersall P.** 2004. A conserved leucine that constricts the pore through the capsid fivefold cylinder plays a central role in parvoviral infection. Virology **323**:243–256.
28. **Hickman AB, Ronning DR, Perez ZN, Kotin RM, Dyda F.** 2004. The nuclease domain of adeno-associated virus Rep coordinates replication initiation using two distinct DNA recognition interfaces. Mol. Cell **13**: 403–414.
29. **Im DS, Muzyczka N.** 1989. Factors that bind to adeno-associated virus terminal repeats. J. Virol. **63**:3095–3104.
30. **Kaul S, Blackford JA, Chen J, Ogryzko VV, Simons SS.** 2000. Properties of the glucocorticoid modulatory element binding proteins GMEB-1 and -2: potential new modifiers of glucocorticoid receptor transactivation and members of the family of KDWK proteins. Mol. Endocrinol. **14**:1010–1027.
31. **Kestler J, et al.** 1999. cis requirements for the efficient production of recombinant DNA vectors based on autonomous parvoviruses. Hum. Gene Ther. **10**:1619–1632.
32. **Kotin RM, Linden RM, Berns KI.** 1992. Characterization of a preferred site on human chromosome 19q for integration of adeno-associated virus DNA by non-homologous recombination. EMBO J. **11**:5071–5078.
33. **Linden RM, Ward P, Giraud C, Winocour E, Berns KI.** 1996. Site-specific integration by adeno-associated virus. Proc. Natl. Acad. Sci. U. S. A. **93**:11288–11294.
34. **López-Bueno A, Mateu MG, Almendral JM.** 2003. High mutant frequency in populations of a DNA virus allows evasion from antibody therapy in an immunodeficient host. J. Virol. **77**:2701–2708.
35. **Paglino J, Burnett E, Tattersall P.** 2007. Exploring the contribution of

distal P4 promoter elements to the oncoselectivity of minute virus of mice. Virology **361**:174–184.
36. **Perros M, et al.** 1995. Upstream CREs participate in the basal activity of minute virus of mice promoter P4 and in its stimulation in ras-transformed cells. J. Virol. **69**:5506–5515.
37. **Ryan JH, Zolotukhin S, Muzyczka N.** 1996. Sequence requirements for binding of Rep68 to the adeno-associated virus terminal repeats. J. Virol. **70**:1542–1553.
38. **Tattersall P, Crawford LV, Shatkin AJ.** 1973. Replication of the parvovirus MVM. II. Isolation and characterization of intermediates in the replication of the viral deoxyribonucleic acid. J. Virol. **12**:1446–1456.
39. **Tijssen P, et al.** 2011. Parvoviridae, p 375–395. *In* King AMQ, Adams MJ, Carstens E, Lefkowitz EJ (ed), Virus taxonomy: classification and nomenclature of viruses. Ninth report of the International Committee on Taxonomy of Viruses. Elsevier, San Diego, CA.
40. **Willwand K, Hirt B.** 1993. The major capsid protein VP2 of minute virus of mice (MVM) can form particles which bind to the 3′-terminal hairpin of MVM replicative-form DNA and package single-stranded viral progeny DNA. J. Virol. **67**:5660–5663.
41. **Willwand K, Hirt B.** 1991. The minute virus of mice capsid specifically recognizes the 3′ hairpin structure of the viral replicative-form DNA: mapping of the binding site by hydroxyl radical footprinting. J. Virol. **65**:4629–4635.
42. **Yeung DE, et al.** 1991. Monoclonal antibodies to the major nonstructural nuclear protein of minute virus of mice. Virology **181**:35–45.